Communication: Four-component density matrix renormalization group

Stefan Knecht, Örs Legeza, and Markus Reiher

Citation: The Journal of Chemical Physics **140**, 041101 (2014); doi: 10.1063/1.4862495
View online: http://dx.doi.org/10.1063/1.4862495
View Table of Contents: http://aip.scitation.org/toc/jcp/140/4
Published by the American Institute of Physics

Communication: Four-component density matrix renormalization group

Stefan Knecht,[1,a)] Örs Legeza,[2,b)] and Markus Reiher[1,c)]
[1]*ETH Zürich, Laboratory of Physical Chemistry, Vladimir-Prelog-Weg 2, 8093 Zürich, Switzerland*
[2]*Strongly Correlated Systems "Lendület" Research Group, Wigner Research Center for Physics, H-1525 Budapest, Hungary*

(Received 3 December 2013; accepted 6 January 2014; published online 22 January 2014)

We present the first implementation of the relativistic quantum chemical two- and four-component density matrix renormalization group algorithm that includes a variational description of scalar-relativistic effects and spin–orbit coupling. Numerical results based on the four-component Dirac–Coulomb Hamiltonian are presented for the standard reference molecule for correlated relativistic benchmarks: thallium hydride. © *2014 AIP Publishing LLC*. [http://dx.doi.org/10.1063/1.4862495]

Owing to remarkable advances in the past decades, relativistic quantum chemical methods have become a routinely applicable and indispensable tool for the accurate description of the chemistry and spectroscopy of heavy-element compounds[1–3] and even of first- and second-row molecules.[4] Major challenges for relativistic quantum chemistry originate from (i) the reduction of non-relativistic (spin and spatial) symmetries caused by magnetic couplings that lead to in general complex wave functions and require the use of double-group symmetry as well as (ii) the large number of (unpaired) valence electrons to be correlated (in particular for heavy elements) and (iii) the occurrence of near-degeneracies of electronic states. Popular quantum chemical methods such as CASSCF/CASPT2/SO-CASPT2[5] assume an additivity of electron correlation and spin–orbit effects or a weak polarization of orbitals due to spin–orbit interaction, or both. Hence, for heavy-element compounds accuracy is inevitably limited as relativistic effects and static or dynamic electron correlation are often not only large but also counteracting.[1,6]

To address the latter issue adequately, a number of genuine relativistic multiconfigurational and multireference approaches have been proposed.[7–9] In this Communication we merge the strengths of the density matrix renormalization group (DMRG) algorithm,[10] which has been successfully introduced to the field of non-relativistic quantum chemistry,[11–13] with a variational description of all relativistic effects in the orbital basis. This new four-component (4c) DMRG *ansatz* goes beyond preceding scalar-relativistic DMRG approaches[14,15] and allows us to efficiently describe first and foremost non-dynamic correlation (or strong correlations) in heavy-element complexes by means of extensive active orbital spaces which would surmount capabilities of any to-date available relativistic multiconfigurational approach.

Our relativistic DMRG implementation rests on the time-independent, first-quantized 4c-Dirac–Coulomb(–Breit) Hamiltonian[16] – any two-component (2c) Hamiltonian is also directly usable – (with positive-energy projectors omitted for brevity),[2,3]

$$\hat{H}_{el} = \sum_i \hat{h}_D(i) + \frac{1}{2}\sum_{i\neq j} \hat{g}(i,j) + V_{NN}, \tag{1}$$

where $\hat{h}_D(i)$ is the one-electron Dirac Hamiltonian for electron i, $\hat{g}(i,j)$ is a two-electron operator describing the interaction between electrons i and j, and V_{NN} is the classical nuclear repulsion energy operator. In the absence of any external magnetic field it can be shown that Eq. (1) is symmetric under time-reversal[3] from which follows that a fermion four-component spinor function ϕ_i occurs in Kramers pairs $\{\phi_i, \bar{\phi}_i\}$. A spinor $\bar{\phi}_i$ can thus be obtained from the action of the time-reversal operator $\hat{\mathcal{K}} = -i\,\Sigma_y \hat{\mathcal{K}}_0$ on ϕ_i, that is $\hat{\mathcal{K}}\phi_i = \bar{\phi}_i$. Hence, our 4c- (or 2c-)spinor basis is comprised of Kramers pairs.

In the no-pair approximation, we can formulate the resulting Hamiltonian in second-quantized and normal ordered form,

$$\hat{\tilde{H}}_{el} = \sum_{PQ} F_P^Q \{a_P^\dagger a_Q\} + \frac{1}{4}\sum_{PQRS} V_{PR}^{QS} \{a_P^\dagger a_R^\dagger a_S a_Q\}, \tag{2}$$

where the summation indices P, Q, R, S strictly refer to positive-energy spinors, and F_P^Q and $V_{PR}^{QS} = (G_{PR}^{QS} - G_{PR}^{SQ})$ are Fock-matrix elements and antisymmetrized two-electron integrals G_{PR}^{QS}, respectively.

We benefit from a quaternion symmetry scheme[17] that has been implemented for the binary double groups D_{2h}^* and subgroups thereof in the `Dirac` program package which our DMRG program is interfaced. In this scheme, point group symmetry and quaternion operator algebra are combined advantageously such that the eigenvalue equation, Eq. (1), can be solved either using real (double groups D_{2h}^*, D_2^*, and C_{2v}^*; resulting number of non-zero real matrices of a quaternion operator matrix representation: NZ = 1), complex (C_{2h}^*, C_2^*, and C_s^*; NZ = 2), or quaternion algebra (C_i^* and C_1^*; NZ = 4). Working in a Kramers-paired spinor basis, one can then show that all operator matrix elements $t_{p\bar{q}}$ of a time-symmetric one-electron operator $\hat{t}$ are zero by symmetry. Furthermore, the complete set of two-electron integrals G_{PR}^{QS} of the two-electron (Coulomb) operator $\hat{g}$ in molecular spinor (MS)

a)Electronic mail: stefan.knecht@phys.chem.ethz.ch
b)Electronic mail: legeza.ors@wigner.mta.hu
c)Electronic mail: markus.reiher@phys.chem.ethz.ch

basis can be cast into a 4 × 3 ((NZ,3)) matrix representation (see also Appendix B.3 page 161*ff* of Ref. 18),

$$\mathbf{G} = \begin{pmatrix} \mathcal{R}((PQ|RS)) & \mathcal{R}((P\bar{Q}|R\bar{S})) & \mathcal{R}((\bar{P}Q|\bar{R}S)) \\ \mathcal{I}((PQ|RS)) & \mathcal{I}((P\bar{Q}|R\bar{S})) & \mathcal{I}((\bar{P}Q|\bar{R}S)) \\ \mathcal{R}((PQ|R\bar{S})) & \mathcal{R}((P\bar{Q}|RS)) & \mathcal{R}((\bar{P}Q|RS)) \\ \mathcal{I}((PQ|R\bar{S})) & \mathcal{I}((P\bar{Q}|RS)) & \mathcal{I}((\bar{P}Q|RS)) \end{pmatrix}, \quad (3)$$

where $\mathcal{R}$ and $\mathcal{I}$ denote the real and complex parts of a two-electron integral in MS representation, respectively. The number of nonzero rows for a given binary double group thus corresponds to the NZ rank as given above. Important symmetry reductions for both the one- and two-electron integrals are therefore being taken into account in our relativistic Kramers-unrestricted DMRG implementation.

In a Kramers-restricted spinor basis all one-electron matrix elements F_P^Q (see Eq. (2)) among barred and unbarred components will be identical while matrix elements between barred and unbarred are non-zero only in the NZ = 4 case. In contrast, a two-electron integral G_{PR}^{QS} may generally be comprised of barred and unbarred spinors. As illustrated by Eq. (3) for NZ = 1 and NZ = 2, respectively, only an even number ($n_{\text{barred}} = 0, 2, 4$) of barred spinors yields a non-vanishing two-electron integral whereas for NZ = 4 all combinations are contributing. Even though integrals can be made real-valued (NZ = 1), permutational symmetry is reduced by a factor two compared to the 8-fold permutational symmetry in the non-relativistic case since orbitals are complex in a relativistic framework.

In DMRG, electron–electron correlation is taken into account by an iterative procedure that minimizes the Rayleigh quotient corresponding to the electronic Hamiltonian $\tilde{\tilde{H}}$ and eventually converges a full-CI-type wave function within the selected active orbital space. The full configuration Hilbert space of a finite system comprising N MSs, $\Lambda^{(N)}$, is built from tensor product spaces of local orbital (tensor) spaces Λ_i,[19] which can be written as $\Lambda^{(N)} = \otimes_{i=1}^{N} \Lambda_i$. Our implementation exploits a two-dimensional local Hilbert-space representation, $q = 2$, where each spinor can be either empty or singly occupied. The tensor space dimension is then 2^N with N being the number of spinors.

In the two-site DMRG variant,[10] that is the basis for our relativistic DMRG implementation, $\Lambda^{(N)}$ is approximated by a tensor product space of four tensor spaces, i.e., $\Lambda_{\text{DMRG}}^{(N)} = \Lambda^{(l)} \otimes \Lambda_{l+1} \otimes \Lambda_{l+2} \otimes \Lambda^{(r)}$. The dimensions of the corresponding local *left* (l) and *right* (r) spaces are denoted as $M_l = \dim\, \Lambda^{(l)}$ and $M_r = \dim\, \Lambda^{(r)}$, respectively. With $q = \dim\, \Lambda_{l+1} = \dim\, \Lambda_{l+2}$ the resulting dimensionality of the DMRG wave function is $\dim\, \Lambda_{\text{DMRG}}^{(N)} = q^2 M_l M_r \ll q^N$. The number of block states, M_l and M_r, required to achieve sufficient convergence can be regarded as a function of the level of entanglement among the molecular orbitals. Hence the maximum number of block states $M_{\max} = \max(M_l, M_r)$ determines the accuracy of a DMRG calculation.[20]

The success and numerical efficiency of the DMRG algorithm rely on a subsequent application of the singular value decomposition (SVD) theorem[19,21] while the performance depends on the level of entanglement encoded in the wave function.[22] During an SVD step, the finite system is divided into two parts $\Lambda_{\text{DMRG}}^{(N)} = \Lambda^{(s)} \otimes \Lambda^{(e)}$, namely into a system and an environment block. In each DMRG step, the basis states of the system block are then transformed to a new *truncated basis* set by a unitary transformation based on the preceding SVD.[23] This transformation depends therefore on how accurately the environment is represented[24] as well as on the level of truncation.[20] As a consequence the accuracy of the DMRG method is governed by the truncation error, $\delta\varepsilon_{\text{TR}}$, as well as by the environmental error, $\delta\varepsilon_{\text{sweep}}$.[25] The latter is minimized in each DMRG macro-iteration by a successive application of the SVD going through the system back and forth ("sweeping").

In order to minimize $\delta\varepsilon_{\text{sweep}}$, which is usually largest during the initial sweep of the DMRG approach because of a poor representation of the environment, we take advantage of the Configuration Interaction based Extended Active Space procedure (CI-DEAS)[26,27] to efficiently construct the environmental basis states by means of an orbital entropy profile.[28] The latter is dependent on the orbital ordering along a (fictitious) one-dimensional chain[22,29] and determines the maximum number of block states $M_{\max} = \max(M)$ that is needed to satisfy an *a priori* defined accuracy threshold given by a value χ.

The truncation error $\delta\varepsilon_{\text{TR}}$ is a function of the total number of block states M. Assuming $M_l = M_r = M$ we can exploit a second-order polynomial fit as a function of $1/M$ by taking the limit of zero energy change between two sweeps $E_{el}(M, \delta\varepsilon_{\text{sweep}} = 0)$ for a given M to provide a good estimate for the truncation-free solution.[25,30]

We demonstrate the capabilities of our 4c-DMRG implementation at the example of the thallium hydride molecule since this system has become a standard benchmark molecule for a plethora of relativistic methods.[31–40,58] Spinors and MS integrals were computed with a development version of the `Dirac12` program package[41] using the Dirac–Coulomb (DC) Hamiltonian and triple-ζ basis sets for Tl (cv3z)[42,43] and H (cc-pVTZ),[44] which include core-correlating functions for Tl. All DMRG calculations were performed with the relativistic development branch of the QC-DMRG-BUDAPEST program.[45] C_{2v}^* double group symmetry (NZ = 1) was assumed throughout all calculations for TlH. MP2 natural spinors (NSs),[46] correlating the Tl 5*s*5*p*4*f*5*d*6*s*6*p* and H 1*s* electrons while keeping the remaining core electrons of Tl frozen, served as the orbital basis for all electron-correlation calculations. Since `Dirac12` requires to use uncontracted basis sets in a four-component framework, a virtual orbital threshold was set at 135 hartree, such that the initial virtual correlation space in the MP2 calculation comprised all recommended core-valence and valence-correlation functions. The final active space was then chosen to include all occupied spinors that have MP2-NS occupancies less than 1.98 as well as all virtuals up to a cutoff of ≈0.001 in the MP2-NS occupation numbers. Given this criterion, an active space of 14 electrons – the occupied Tl 5*d*6*s*6*p* plus H 1*s* shells – in 47 Kramers pairs (94 spinors) was used in the CI[47–49] MP2, CC,[50,51] and DMRG calculations. The latter are further characterized by the choice of $M_{\max}$, $M_{\min}$, $M_{\min}^{\text{DEAS}}$, and χ, denoted in the following as DMRG(14,94)[$M_{\max}$, $M_{\min}$, $M_{\min}^{\text{DEAS}}$, χ].

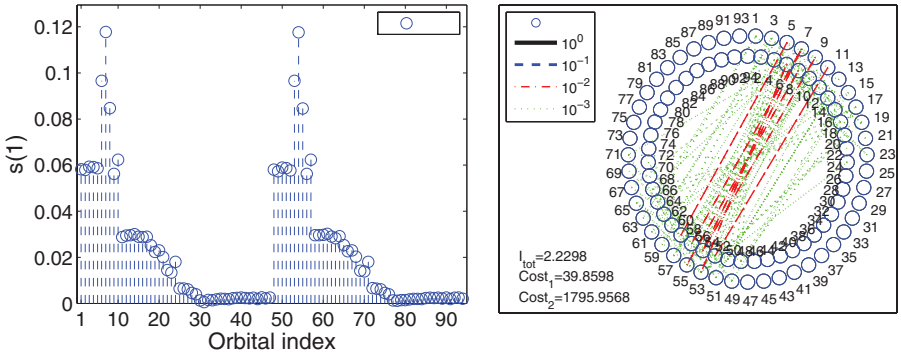

FIG. 1. Left: One-orbital entropy profile, s_i, calculated at the experimental internuclear distance r_e^{exp}=1.872 Å. The larger the entropy value for a given spinor the larger its contribution to the total correlation energy. Right: Schematic plot of a piecewise orbital entanglement based on the two-orbital mutual information, I_{ij}. Entanglement strengths are indicated by different colors.

Figure 1 depicts the one-orbital s_i and two-orbital I_{ij} entropy profiles[22,52,53] at the experimental internuclear distance $r_e^{\text{exp}} = 1.872$ Å computed from an initial DMRG[256,256,256,10^{-5}] calculation. We first note that the one-orbital entropy profile (left-hand side of Figure 1) is nearly perfectly symmetric with respect to the unbarred (#1–#47) and barred (#48–#94) spinors where any slight deviation is an artefact of the preset low M_{min}, M_{max} values. The total quantum information I_{tot} encoded in the wave function, defined as the sum of one-orbital entropies, $I_{\text{tot}} = \sum_i s_i$, can be taken as a measure of the importance of dynamic (weak) electron correlation. The lower I_{tot} (compared to $I_{\text{tot}}^{\text{max}} = \sum_i s_i^{\text{max}} = N \ln(2) = 65.15$), the more important will be an appropriate account of dynamic electron correlation in order to grasp all important correlation effects. In the present case of TlH we have $I_{\text{tot}} \simeq 2.23 \ll I_{\text{tot}}^{\text{max}}$ which points to the fact that TlH is a predominantly single-reference close to its equilibrium structure.

The two-orbital mutual information, I_{ij}, confirms this qualitative picture. I_{ij} values are visualized in the right panel of Figure 1, where the degree of entanglement between spinors is marked by a color-coded connecting line. While few spinors are weakly entangled (red) the majority is entangled with even smaller strengths (green). Since several spinors are mutually entangled with the same order of magnitude, we expect that large M_{min}, M_{max} values combined with a low quantum information loss threshold χ are required to reach a fully converged DMRG wave function.

To corroborate this hypothesis we compiled in Table I total energy differences for various standard wave-function-expansion methods as well as for our 4c-DMRG(14,94)[4500,1024,2048,10^{-5}] model with respect to a chosen 4c-CCSDTQ reference at $r_e^{\text{exp}} = 1.872$ Å. The 4c-DMRG wave function was built from an optimized ordering of orbitals based on the entropy profiles given in Figure 1 and by applying high accuracy settings in the initial CI-DEAS sweep (with $\text{CI}_{\text{level}} = 4$ and $\chi_{\text{CI}} = 10^{-8}$). These initial conditions ensured both a rapid elimination of the environmental error and a fast total convergence towards the global minimum. The 4c-CISDTQ energy is reached after no more than six sweeps of the 4c-DMRG wave function optimization procedure. Inspection of Table I furthermore reveals that the 4c-DMRG energy is, although being below our best variational 4c-CISDTQ energy, still 2.57 mH higher than the reference 4c-CCSDTQ as well as 2.89 mH higher than the single-reference 4c-CCSD(T) energies. We recall that DMRG is best suited for static-correlation problems, whereas TlH is dominated by dynamic correlation. The missing dynamic-correlation contributions may be captured by multireference perturbation theory on top of the relativistic DMRG wave function. However, extrapolating the DMRG energy for a given M to the limit $E_{el}(M, \delta\varepsilon_{\text{sweep}} = 0)$ provides an effective means to eliminate the truncation error. The resulting best estimate of $E_{el}(M \to \infty) = -20275.8395$ H at r_e^{exp}=1.872 Å is then as close as +0.7 mH to the CCSDTQ reference energy. Moreover, we found that even a reduced-M 4c-DMRG[512, $\delta\varepsilon_{\text{sweep}} = 0$] potential energy curve does not only effectively reproduce the shape of the 4c-CCSDTQ potential energy curve but also yields accurate spectroscopic constants—extracted from a fourth-order polynomial fit and compiled in Table II. The 4c-CCSDTQ data are in excellent agreement with experiment for the equilibrium internuclear distance r_e, harmonic frequency ω_e, and for the anharmonicity constant $\omega_e x_e$. Our DMRG results also show an excellent agreement with experiment for r_e, while predicting slightly too high values for ω_e (+20 cm^{-1}) and $\omega_e x_e$ (+4 cm^{-1}), respectively.

TABLE I. Total electronic energy differences ΔE_{el} (in mH) for different correlation approaches with respect to the 4c-CCSDTQ(14,94) reference energy of −20275840.24233 mH for TlH computed at the experimental equilibrium internuclear distance 1.872 Å.

Method	ΔE_{el}
4c-CISD(14,94)	41.55
4-CISDT(14,94)	32.80
4c-CISDTQ(14,94)	2.63
4c-MP2(14,94)	− 13.49
4c-CCSD(14,94)	10.58
4c-CCSD(T)(14,94)	− 0.32
4c-CCSDT(14,94)	0.33
4c-CCSDT(Q)(14,94)	− 0.07
4c-DMRG(14,94)[4500,1024,2048,10^{-5}]	2.57
4c-DMRG(14,94)[$M \to \infty$ extrapolated]	0.7

TABLE II. Spectroscopic constants of ^{205}TlH obtained from 4c-DMRG[512, $\delta\varepsilon_{\text{sweep}} = 0$)], CI, and CC calculations in comparison with other theoretical and experimental work.

Method	r_e (Å)	ω_e (cm^{-1})	$\omega_e x_e$ (cm^{-1})
4c-DMRG(14,94)[512]	1.873	1411	26.64
4c-CISD(14,94)	1.856	1462	23.11
4c-CISDTQ(14,94)	1.871	1405	20.11
4c-MP2(14,94)	1.828	1546	47.27
4c-CCSD(14,94)	1.871	1405	19.36
4c-CCSD(T)(14,94)	1.873	1400	23.52
4c-CCSDT(14,94)	1.873	1398	22.28
4c-CCSDT(Q)(14,94)	1.873	1397	21.01
4c-CCSDTQ(14,94)	1.873	1397	22.24
CCSD(T)[a]	1.876	1385	n/a
CCSD(T)[b]	1.877	1376	n/a
MRD-CI[c]	1.870	1420	n/a
SO-MCQDPT[d]	1.876	1391	29.42
Experiment[e]	1.872	1390.7	22.7

[a]4c-DC CCSD(T) [14 electrons], see Ref. 35.
[b]4c-DC-Gaunt CCSD(T) [36 electrons], see Ref. 35.
[c]GRECP spin–orbit MRD-CI, see Ref. 34.
[d]Model-core potential spin–orbit MCQDPT, see Ref. 40.
[e]Experimental data taken from Refs. 34 and 55–57.

We conclude with a note on the computational demands of our 4c-DMRG implementation in comparison to CCSDTQ. The benchmark DMRG[4500,1024,2048,10^{-5}] calculation required ≈50 GB of core memory to represent all operators of the left and right blocks of the most expensive local optimization step while the relativistic MRCC code[54] had similar memory requirements for the optimization of the various t amplitudes.

Our new 4c- and 2c-DMRG approach (no 2c-results shown here) bears the potential to become a new powerful tool for the theoretical chemistry and photophysics of heavy-element molecules dominated by strong static electron correlation as observed, for instance, in lanthanide and actinide complexes.

M.R. has been financially supported by SNF (No. 200020_144458/1) and O.L. by OTKA (Nos. K100908 and NN110360).

[1]J. Autschbach, J. Chem. Phys. **136**, 150902 (2012).
[2]K. G. Dyall and K. Fægri, *Introduction to Relativistic Quantum Chemistry* (Oxford University Press, Oxford, 2007).
[3]M. Reiher and A. Wolf, *Relativistic Quantum Chemistry* (Wiley-VCH, Weinheim, 2009).
[4]C. M. Marian, WIREs Comput. Mol. Sci. **2**, 187 (2012).
[5]D. Roca-Sanjuan, F. Aquilante, and R. Lindh, WIREs Comput. Mol. Sci. **2**, 585 (2012).
[6]P. Pyykkö, Chem. Rev. **88**, 563 (1988).
[7]T. Fleig, Chem. Phys. **395**, 2 (2012).
[8]D. Ganyushin and F. Neese, J. Chem. Phys. **138**, 104113 (2013).
[9]I. Kim and Y. S. Lee, J. Chem. Phys. **139**, 134115 (2013).
[10]S. R. White, Phys. Rev. Lett. **69**, 2863 (1992).
[11]Ö. Legeza, R. Noack, J. Sólyom, and L. Tincani, *Computational Many-Particle Physics*, Lecture Notes in Physics Vol. 739, edited by H. Fehske, R. Schneider, and A. Weibe (Springer, Berlin, 2008), pp. 653–664.
[12]K. H. Marti and M. Reiher, Z. Phys. Chem. **224**, 583 (2010).
[13]G. K.-L. Chan and S. Sharma, Annu. Rev. Phys. Chem. **62**, 465 (2011).
[14]P. Tecmer, K. Boguslawski, Ö. Legeza, and M. Reiher, Phys. Chem. Chem. Phys. **16**, 719 (2014).
[15]G. Moritz, A. Wolf, and M. Reiher, J. Chem. Phys. **123**, 184105 (2005).
[16]T. Saue, Chem. Phys. Chem. **12**, 3077 (2011).
[17]T. Saue and H. J. A. Jensen, J. Chem. Phys. **111**, 6211 (1999).
[18]J. Thyssen, Ph.D. thesis, University of Southern Denmark, 2001.
[19]Ö. Legeza, T. Rohwedder, R. Schneider, and S. Szalay, "Tensor product approximation (DMRG) and coupled cluster method in quantum chemistry," preprint arXiv:1310.2736 (2013).
[20]Ö. Legeza, J. Röder, and B. A. Hess, Phys. Rev. B **67**, 125114 (2003).
[21]U. Schollwöck, Ann. Phys. **326**, 96 (2011).
[22]Ö. Legeza and J. Sólyom, Phys. Rev. B **70**, 205118 (2004).
[23]U. Schollwöck, Rev. Mod. Phys. **77**, 259 (2005).
[24]G. Moritz and M. Reiher, J. Chem. Phys. **124**, 034103 (2006).
[25]Ö. Legeza and G. Fáth, Phys. Rev. B **53**, 14349 (1996).
[26]Ö. Legeza and J. Sólyom, Phys. Rev. B **68**, 195116 (2003).
[27]Ö. Legeza and J. Sólyom, see www.itp.uni-hannover.de/~jeckelm/dmrg/workshop/proceedings.html.
[28]G. Barcza, Ö. Legeza, K. H. Marti, and M. Reiher, Phys. Rev. A **83**, 012508 (2011).
[29]G. Moritz, B. Hess, and M. Reiher, J. Chem. Phys. **122**, 024107 (2005).
[30]G. Barcza, Ö. Legeza, M. R. Noack, and J. Sólyom, Phys. Rev. B **86**, 075133 (2012).
[31]L. Seijo, J. Chem. Phys. **102**, 8078 (1995).
[32]E. van Lenthe, J. G. Snijders, and E. J. Baerends, J. Chem. Phys. **105**, 6505 (1996).
[33]Y.-K. Han, C. Bae, and Y. S. Lee, J. Chem. Phys. **110**, 9353 (1999).
[34]A. V. Titov, N. S. Mosyagin, A. B. Alekseyev, and R. J. Buenker, Int. J. Quantum Chem. **81**, 409 (2001).
[35]K. Fægri and L. Visscher, Theor. Chem. Acc. **105**, 265 (2001).
[36]M. Mayer, S. Krüger, and N. Rösch, J. Chem. Phys. **115**, 4411 (2001).
[37]Y. J. Choi, Y.-K. Han, and Y. S. Lee, J. Chem. Phys. **115**, 3448 (2001).
[38]M. Ilias, V. Kellö, L. Visscher, and B. Schimmelpfennig, J. Chem. Phys. **115**, 9667 (2001).
[39]Y. J. Choi and Y. S. Lee, J. Chem. Phys. **119**, 2014 (2003).
[40]T. Zeng, D. G. Fedorov, and M. Klobukowski, J. Chem. Phys. **132**, 074102 (2010).
[41]DIRAC12 (2012), see www.diracprogram.org for further information.
[42]K. G. Dyall, Theor. Chem. Acc. **108**, 335 (2002); **109**, 284 (2003), erratum; **115**, 441 (2006), revision.
[43]K. G. Dyall, Theor. Chem. Acc. **131**, 1217 (2012).
[44]T. H. Dunning, Jr., J. Chem. Phys. **90**, 1007 (1989).
[45]Ö. Legeza, QC-DMRG-BUDAPEST, *2000–2013, HAS Wigner Budapest.*
[46]Option .MP2 NO in the wave function section of `Dirac12`.
[47]T. Fleig, J. Olsen, and L. Visscher, J. Chem. Phys. **119**, 2963 (2003).
[48]T. Fleig, H. J. Aa. Jensen, J. Olsen, and L. Visscher, J. Chem. Phys. **124**, 104106 (2006).
[49]S. Knecht, H. J. Aa. Jensen, and T. Fleig, J. Chem. Phys. **132**, 014108 (2010).
[50]MRCC, a string-based quantum chemical program suite written by M. Kállay. See also Ref. 51 as well as http://www.mrcc.hu/.
[51]M. Kállay and P. R. Surján, J. Chem. Phys. **115**, 2945 (2001).
[52]K. Boguslawski, P. Tecmer, Ö. Legeza, and M. Reiher, J. Phys. Chem. Lett. **3**, 3129 (2012).
[53]K. Boguslawski, P. Tecmer, G. Barcza, Ö. Legeza, and M. Reiher, J. Chem. Theory Comput. **9**, 2959 (2013).
[54]M. Kallay, H. Nataraj, B. Sahoo, B. Das, and L. Visscher, Phys. Rev. A **83**, 030503(R) (2011).
[55]B. Grundström and P. Valberg, Z. Phys. **108**, 326 (1938).
[56]*Molecular Spectra and Molecular Structure Constants of Diatomic Molecules*, edited by K. Huber and G. Herzberg (Van Nostrand, New York, 1979).
[57]R.-D. Urban, A. H. Bahnmaier, U. Magg, and H. Jones, Chem. Phys. Lett. **158**, 443 (1989).
[58]M. Seth, P. Schwerdtfeger, and K. Fœgri, J. Chem. Phys. **111**, 6422 (1999).